J. Synchrotron Rad. (1995). **2**, 308–311

Microfocus X-ray Diffraction of Spherulites of Poly-3-hydroxybutyrate

A. Mahendrasingam,[a] C. Martin,[a] W. Fuller,[a] D. J. Blundell,[b] D. MacKerron,[b] R. J. Rule,[c] R. J. Oldman,[c] J. Liggat,[d] C. Riekel[e] and P. Engström[e]

[a]Department of Physics, Keele University, Keele, Staffordshire ST5 5BG, UK, [b]ICI Films, PO Box No. 90, Wilton Centre, Middlesbrough, Cleveland TS6 8JE, UK, [c]ICI Chemicals and Polymers Ltd, PO Box No. 8, The Heath, Runcorn, Cheshire WA7 4QD, UK, [d]Zeneca Bio Products, PO Box No. 2, Billingham, Cleveland TS23 1YN, UK, and [e]ESRF, BP 220, F-38043 Grenoble CEDEX, France

(*Received 9 June 1995; accepted 18 July 1995*)

The microfocus X-ray beamline at the European Synchrotron Radiation Facility has been used to investigate the variation in molecular orientation and crystallinity in spherulites of the organic polymer poly-3-hydroxybutyrate (PHB). This is the first report of the correlation of optical and X-ray measurements on spherulitic polymer films where X-ray diffraction patterns have been recorded and displayed continuously in real time while the specimen was tracked in steps of 10 μm across an incident X-ray beam with a diameter as small as 10 μm.

Keywords: spherulites; X-ray diffraction; microfocus; polymers; PHB.

1. Introduction

X-ray diffraction provides one of the most powerful techniques for the investigation of polymer conformation and organization within partially ordered materials. From optical microscopy it is clear that the direction of molecular orientation within many polymer materials varies over dimensions much smaller than the ~100 μm beam diameter available from conventional rotating-anode X-ray sources and even from second-generation synchrotron radiation sources. The studies described here demonstrate that by exploiting the high degree of collimation and beam stability of the European Synchrotron Radiation Source (ESRF), together with microfocusing optics, it is possible to characterize the variation in molecular orientation and crystallinity within polymer materials with a spatial resolution as small as 10 μm. The dramatic gains offered by the ESRF in conjunction with a CCD detector system and a high-precision computer-controlled *X*/*Z* stage are well illustrated by comparing the observations recorded in the experiments described here with those recorded in studies of crystallite orientation in spherulites using a conventional X-ray source and photographic recording (Barham, Keller, Otun & Holmes, 1984; Fujiwara, 1960).

The homopolymer poly-D-(–)-3-hydroxybutyrate (PHB) used for this study is one of the series of optically active thermoplastic polymers made under the commercial name 'Biopol' by Zeneca Bio Products. It is produced by a wide variety of micro-organisms, being used in these organisms for energy and carbon storage. The biological rather than the petroleum origins of 'Biopol', its biodegradability, and its ability to form films with the properties of conventional thermoplastics give it technological importance as well as fundamental interest (Holmes, 1988). The purity of this polymer leads to an absence of heterogeneous nuclei and gives it the capacity to form large spherulites of high crystallinity.

2. Experimental techniques

The microfocus instrumentation on beamline ID13 at the ESRF can provide a highly monochromatic X-ray beam with a wavelength of 0.92 Å and a photon flux of $\sim 10^{11}$ photons s^{-1} in a beam diameter at the specimen of ~7 μm FWHM (Engström, Fiedler & Riekel, 1995). Crucial to the experiments described here was the availability of a computer-controlled *X*/*Y* stage which allowed the specimen to be tracked in two dimensions perpendicular to the X-ray beam in steps as small as 1 μm. The backlash in this device was negligibly small so that a specimen could be returned to its original position with respect to the X-ray beam with an accuracy of *ca* 0.1 μm. X-ray diffraction data were recorded using a Photonics Science CCD detector with a sensitive area of 92 × 69 mm and an effective pixel area of 120 × 120 μm. The specimen–detector distance could be as small as 6 cm. At this distance diffraction data could be recorded for *d* spacings from 15 to 1.5 Å.

Diffraction patterns were recorded with exposure times of 40 ms. Over this period, the pattern was integrated within the detector in 8-bit pixels before being captured by a Synoptic i860 framegrabber. In order to improve the statistics of the diffraction data, the framegrabber allowed further integration of successive diffraction patterns. In the

studies described here, typically 25 frames (*i.e.* the number recorded during 1 s) were integrated before the resultant composite frame was downloaded to the hard disk of a 486 PC through a SCSI interface. Because of the time required to download this 0.8 MB file, there was a dead time of ~1 s before the framegrabber could capture further data from the CCD. However, in parallel with the transfer of data to the framegrabber, the signal accumulated in the CCD during each 40 ms was written to a standard VCR video recorder using VHS format. Although data recorded on video tape have limitations for accurate determination of structure-factor amplitudes in a detailed X-ray structural refinement, the video recorder image is more than adequate for determining the degree and direction of molecular orientation and has the advantage of providing a display in real time which monitors the variation in the diffraction pattern with the standard 25 Hz time resolution of a TV display.

The ability to record and display in real time the variation in the diffraction pattern, and hence in the structure of the specimen, was central to the success of these investigations since it allowed decisions on stepping the specimen across the X-ray beam to be made with the minimum of time delay. A typical experiment aimed at monitoring structural variation across an area of 1 × 1 mm at a spatial resolution of ~10 μm would generate 10 000 frames and present formidable problems if these were to be analysed manually. We have therefore developed software which allows the variation in orientation and crystallinity in a sequence of frames to be determined automatically, and this variation, and the patterns from which it is derived, to be mapped in ways that allow ready comparison with optical microscope images of birefringence variation across the specimen.

In order to relate optical and X-ray observations, two wires were placed on the specimen to provide reference axes with respect to which the coordinates of optically significant features in the specimen could be determined with an accuracy of ~1 μm. The position of the specimen was adjusted with respect to the incident X-ray beam by tracking the specimen stage until the geometrical shadow within the parasitic scatter on the detector of the two reference wires was centred on that of the backstop. Knowing the coordinates of any optical feature in the specimen with respect to the two reference wires it was possible to translate the specimen until the feature was located in the X-ray beam.

3. Results

Films of the polymer (M_W = 790 000 g mol^{-1}, M_W/M_n = 3.1, T_m = 451 K) were prepared by melting a small quantity of polymer powder (~1 mg) between two glass cover-slips on a hot stage at 473 K. After gently pressing the cover-slips together to ensure an even melt film, the hot-stage was cooled at 40 K min^{-1} to 353 K, at which temperature the low rate of homogeneous nucleation allowed the growth of spherulites several millimeters in diameter. From the optical microscope image of the specimen in Fig. 1 it can be seen that the film is rich in spherulitic structures. The film thickness is much less than the diameters of

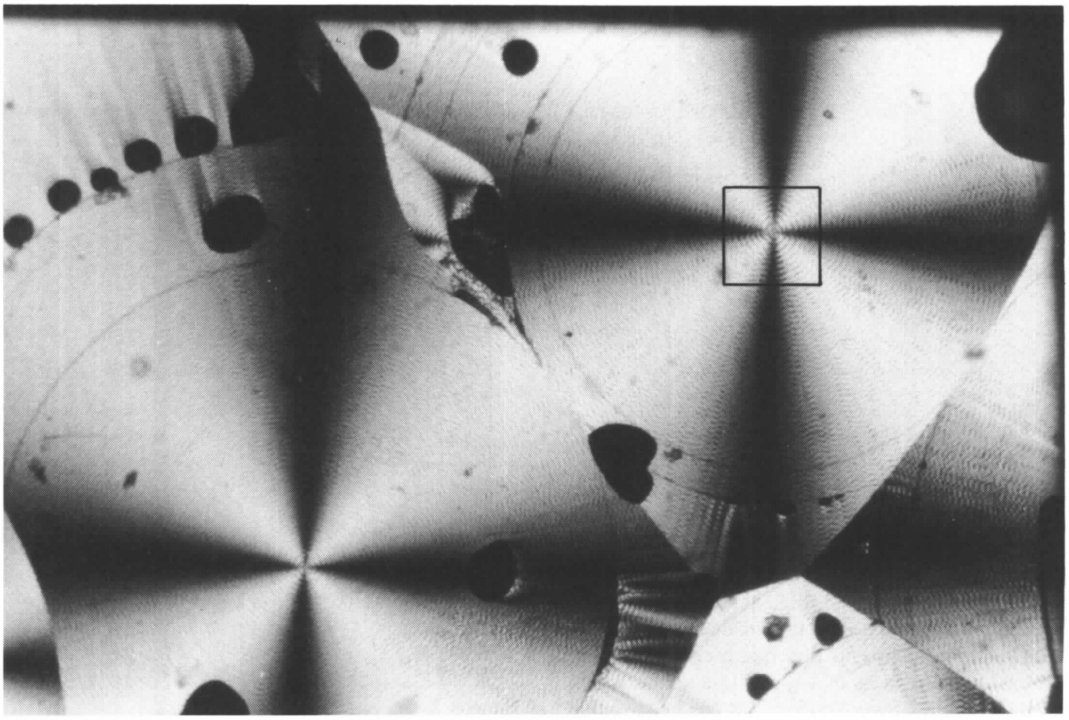

Figure 1
Polarizing microscope image of a spherulitic specimen of poly-D-(–)-3-hydroxybutyrate. The X-ray diffraction data described in this paper were recorded from the region within the square frame 150 × 150 μm drawn around the centre of one of the spherulites in this figure.

typical spherulites which are therefore constrained in their development so that away from their nuclei they become essentially two-dimensional objects with little overlap in the direction of the incident X-ray beam. The spherulite selected for detailed X-ray analysis is indicated in Fig. 1. X-ray diffraction patterns were recorded as the specimen was stepped across a square net of area 150 × 150 μm, centred on the centre of the spherulite, in horizontal and vertical steps of 10 μm.

The 15 × 15 diffraction patterns recorded in this way are assembled as a two-dimensional array in Fig. 2. The crystallite orientation in these patterns can readily be related to the patterns previously reported from the same polymer by Barham *et al.* (1984), which they obtained with some difficulty from a large spherulite using a conventional X-ray source. Fig. 3 shows one of the frames taken from Fig. 2 enlarged with the main reflections indexed. It is identical to the pattern reported by Barham *et al.* (1984) and is consistent with the average pattern of many crystal lamellae growing radially along the crystallographic *a* axis, where the *b* and *c* axes systematically rotate around the *a* axis. The array of patterns in Fig. 2 vividly demonstrates that on a spatial resolution of 10 μm, the crystals are systematically oriented with the *a* axis along the radius. It will be noted that patterns at the centre of the array corresponding to the central region of the spherulite have lost the clear *a*-axis orientation and are less distinct. This will be partly due to the specific structure of the nucleus at the centre of the spherulite and to the greater predominance of crystals radiating in directions out of the plane of the sample.

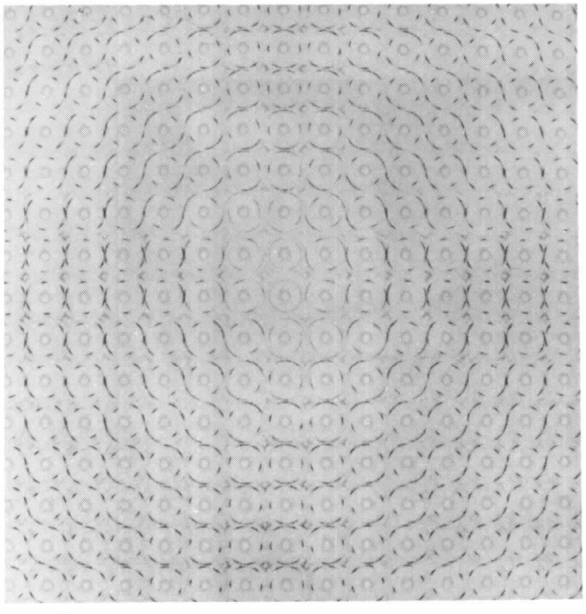

Figure 2
X-ray fibre diffraction patterns recorded from the region of the specimen within the square frame in Fig. 1. Each diffraction pattern was recorded from an area ~10 μm in diameter and the position of the diffraction patterns in this figure corresponds to the relative positions of the regions of the specimen from which they were recorded. From this figure and Fig. 3 it can be seen that each crystallite is oriented so that its *a* axis lies along a radius of the spherulite but that the degree of orientation decreases towards the centre of the spherulite.

4. Conclusions

The high degree of spatial resolution available on the microfocus beamline ID13 at the ESRF has allowed the variation in degree and direction of molecular orientation inferred from optical microscopy and earlier X-ray studies with conventional sources to be confirmed and extended. The ability to monitor effects such as the loss of orientation with diminishing distance from the centre of the spherulite is of particular interest for models of spherulite nucleation and growth. However, this will require more extensive characterization of specimens than has been possible in the preliminary studies described here which were aimed primarily at developing the microfocus facility in ways which can be expected to have wide applicability not only in wide-angle X-ray scattering studies but also in complementary small-angle scattering studies (Snigerev *et al.*, 1994). Furthermore, because the high brilliance of the ESRF allows diffraction data to be collected with exposures as short as 40 ms, even for incident beam diameters of ~10 μm there is a possibility of performing time-resolved studies of structural changes during heating and cooling.

This work was supported by SERC grants GR/J/01950 and GR/H/67966. The work also benefited from exploratory studies on beamline ID13 supported by SERC grant GR/J/57797 to V. T. Forsyth, AM and WF and an allocation of beam time by the ESRF. Much of the equipment used in this study was assembled and commissioned in the Keele Physics Department. We are grateful to D. Bowyer, M. Daniels, M. G. Davies, G. Dudley, E. J. T. Greasley, G.

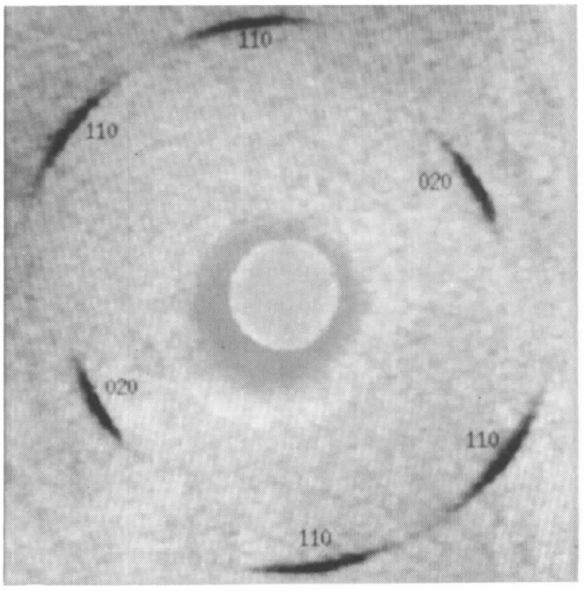

Figure 3
Enlargement of one of the X-ray fibre diffraction patterns in Fig. 2 indicating the indices of the principal reflections. The unit cell is orthorhombic with a = 5.76, b = 13.20, c = 5.96 Å.

Marsh, H. Moors and M. Wallace for technical support and help with preparation of the manuscript.

References

Barham, P. J., Keller, A., Otun, E. L. & Holmes, P. A. (1984). *J. Mater. Sci.* **19**, 2781–2794.

Engström, P., Fiedler, S. & Riekel, C. (1995). *Rev. Sci. Instrum.* **66**, 1348–1350.

Fujiwara, Y. (1960). *J. Appl. Polym. Sci.* **4**, 10–15.

Holmes, P. A. (1988). *Developments in Crystalline Polymers 2*, edited by D. C. Bassett. Amsterdam: Elsevier.

Snigerev, A. A., Snigereva, I. I., Riekel, C., Miller, A., Wess, L. & Wess, T. (1994). *J. Phys. (Paris)*, **3**(C8), 443–446.

J. Synchrotron Rad. (1995). **2**, 312–314

Photoemission Study of CO Adsorption on Gd

C. Searle,[a] R. I. R. Blyth,[a] R. G. White,[b] N. P. Tucker,[a] M. H. Lee[a] and S. D. Barrett[b]

[a]Surface Science Research Centre, University of Liverpool, PO Box 147, Liverpool L69 3BX, UK, and [b]Department of Physics, University of Liverpool, PO Box 147, Liverpool L69 3BX, UK

(*Received 25 April 1995; accepted 14 August 1995*)

Angle-resolved UV photoemission spectroscopy has been used to investigate the interaction of CO with Gd films, grown on W(110). The results suggest that CO adsorbs dissociatively, initially forming Gd_2O_3, with subsequent catalytic oxidation of CO to form carbonate.

Keywords: photoemission; CO on Gd/W(110); angle-resolved UV photoemission spectroscopy; LEED.

1. Introduction

There has been much recent photoemission work (Li, Zhang, Dowben & Onellion, 1993; Vescovo, Rader, Kachel, Alkemper & Carbone, 1993; Navas, Starke, Laubschat, Weschke & Kaindl, 1993) on rare-earth thin films grown on the (110) surfaces of refractory metals, particularly W. These films are crystalline, and yield low-energy electron diffraction (LEED) patterns with hexagonal symmetry. By convention, these films are described as (0001) surfaces, implying an h.c.p. structure. However, this designation is provisional since qualitative LEED cannot determine three-dimensional structure. The majority of rare-earth thin-film studies have been of the clean surfaces; there have been very few studies of the interaction of adsorbates with single-crystal rare-earth surfaces. Early studies of adsorption on rare-earth metal surfaces were motivated by the large hydrogen uptake of these metals, with a parallel interest in possible catalytic applications. Studies were largely of evaporated polycrystalline films, and used combinations of work-function methods (Surplice & Brearley, 1978; Strasser, Bertel & Netzer, 1983) and UV photoemission (Netzer & Bertel, 1982). This paper presents the results of synchrotron radiation photoemission studies for low exposures of CO adsorbed onto Gd/W(110).

2. Experimental

The experiment was performed on the Liverpool/Manchester photoemission beamline (4.1) (Dhanak, Robinson, van der Laan & Thornton, 1992) at the SRS, Daresbury Laboratory. A Vacuum Science Workshop HA54 hemispherical analyser was used, with an overall resolution at $h\nu$ = 40 eV of 0.2 eV. The vacuum chamber, with a base pressure $< 10^{-10}$ mbar, was fitted with Vacuum Generators LEED optics. The W(110) substrate was prepared by roasting at 1400 K in 10^{-6} mbar oxygen to remove carbon, followed by periodic flashing to > 2000 K to remove residual O and H, until the surface showed a sharp 1 × 1 LEED pattern. Cleanliness of the surface was verified by measuring the W $4f_{7/2}$ surface core-level shift, which is known to be highly sensitive to contamination (Riffe, Wertheim & Citrin, 1989).

Gd was evaporated from a water-cooled W-wire evaporator (Dowben, LaGraffe & Onellion, 1989) with the substrate held at room temperature to ensure layer-by-layer growth (Kolaczkiewicz & Bauer, 1986). The pressure remained below 4×10^{-10} mbar during evaporation. Film growth was monitored by UV photoemission spectroscopy until features from the substrate valence band were not detectable. CO (Gas Distillers, 99.997% pure) was dosed by backfilling the chamber, with the gas purity checked using a Vacuum Generators residual gas analyser.

3. Results and discussion

A spectrum from a Gd film (as grown) is shown in Fig. 1. This is in good agreement with previously published spectra of Gd on W(110) (Li *et al.*, 1993). The sharp peak (0.5 eV FWHM) near the Fermi level (E_F) is attributed to a surface state, with its intensity indicating the single-crystal nature of the film. The properties of the surface state have been thoroughly reviewed by Vescovo *et al.* (1993). The 8.4 eV peak is due to emission from the Gd 4*f* states and has a FWHM of 1.5 eV. The nature of the valence-band feature at 1.6–1.7 eV is disputed; while Vescovo *et al.* (1993) consider the feature to be due to a surface resonance, Li *et al.* (1993) assign the emission to Gd 5*d* bulk bands. The peak at 5.8 eV is attributed to oxygen 2*p* orbitals from residual contamination. By comparison with the oxygen-dosing results of Vescovo *et al.* (1993), we estimate the level of oxygen contamination to be <3%.

Fig. 2 shows a series of spectra for a Gd film dosed with CO at room temperature. Spectra for the CO exposure sequence (Fig. 2) show no features with binding energy